Monthly Notices of the ROYAL ASTRONOMICAL SOCIETY

MNRAS **521,** L85–L89 (2023) https://doi.org/10.1093/mnrasl/slad025
Advance Access publication 2023 February 22

The cosmic timeline implied by the *JWST* high-redshift galaxies

Fulvio Melia ★

Department of Physics, The Applied Math Program, and Department of Astronomy, The University of Arizona, AZ 85721, Tucson, USA

Accepted 2023 February 20. Received 2023 February 16; in original form 2022 December 30

ABSTRACT

The so-called impossibly early galaxy problem, first identified via the *Hubble Space Telescope*'s observation of galaxies at redshifts $z > 10$, appears to have been exacerbated by the more recent *JWST* discovery of galaxy candidates at even higher redshifts ($z \sim 17$) which, however, are yet to be confirmed spectroscopically. These candidates would have emerged only ∼230 Myr after the big bang in the context of Lambda cold dark matter (ΛCDM), requiring a more rapid star formation in the earliest galaxies than appears to be permitted by simulations adopting the concordance model parameters. This time-compression problem would therefore be inconsistent with the age–redshift relation predicted by ΛCDM. Instead, the sequence of star formation and galaxy assembly would confirm the timeline predicted by the $R_{\rm h} = ct$ universe, a theoretically advanced version of ΛCDM that incorporates the 'zero active mass' condition from general relativity. This model has accounted for many cosmological data better than ΛCDM, and eliminates all of its inconsistencies, including the horizon and initial entropy problems. The latest *JWST* discoveries at $z \gtrsim 14$, if confirmed, would add further support to the idea that the $R_{\rm h} = ct$ universe is favoured by the observations over the current standard model.

Key words: stars: Population III – galaxies: formation – galaxies: high-redshift – large-scale structure of the Universe – cosmology: observations – cosmology: theory.

1 INTRODUCTION

A surprising number of high-redshift galaxy candidates ($z > 12$) have already been discovered by *JWST* in just the first few weeks of operation (see Table 1). Identified through the Early Release Observations (Pontoppidan et al. 2022), the Cosmic Evolution Early Release Science (CEERS; Finkelstein et al. 2022), and Through the Looking GLASS (GLASS-*JWST*; Treu et al. 2022) science programmes, many of them surpass the distance record previously set at $z = 11.1$ by the *Hubble Space Telescope* (*HST*; Oesch et al. 2016). This is certainly true of candidates up to $z \sim 13$, whose redshift has been confirmed spectroscopically (Robertson et al. 2022).

But the fact that some of these well-formed $\sim 10^9\,{\rm M}_{\odot}$ structures (at $z \sim 16$–17) appear to have emerged only ∼230 Myr after the big bang contrasts with their predicted formation in the standard model of cosmology, which we here take to be Lambda cold dark matter (ΛCDM) with the *Planck* optimized parameters: a Hubble constant, $H_0 = 67.4 \pm 0.5\,{\rm km\,s^{-1}\,Mpc^{-1}}$, a matter density $\Omega_{\rm m} = 0.315 \pm 0.007$, scaled to today's critical density ($\equiv 3c^2H_0^2/8\pi G$), and a spatial curvature constant, $k \approx 0$ (Planck Collaboration VI 2020). In discussing this 'impossibly early galaxy' problem (Melia 2014, 2020), two principal issues typically emerge. The first is whether the gas budget in the early Universe, notably the fraction of baryons condensed within an assumed dark matter halo distribution, was sufficient to account for this high-z galaxy demographic (Behroozi & Silk 2018). The answer could be yes (Donnan et al. 2023), as long as all of the available baryonic gas in haloes was converted into stars. The $z \sim 16$–17 galaxy candidates fall close to the ΛCDM limit, but do not exceed it.

The second concerns whether the dynamics of structure formation could account for the highly compressed timeline implied by these discoveries (for the most recent work on this topic, see Haslbauer et al. 2022; Inayoshi et al. 2022; Kannan et al. 2022; Keller et al. 2023; Yajima et al. 2022; Mirocha & Furlanetto 2023; Whitler et al. 2023). It is the dynamics, of course, coupled to the physical processes responsible for cooling the gas, that would have governed how quickly stars could condense and assemble into billion solar mass structures. One must also fold into this discussion how the 'stellar age' of the high-z sources (column 5 in Table 1) should be interpreted. An examination of the galaxy age versus star formation activity at $z > 8$ (Furtak et al. 2023; Whitler et al. 2023) suggests that the young stellar populations producing much of the current luminosity are built upon older components that formed at $z > 15$, and are being observed during bursts of star formation.

2 HIGH-z GALAXIES IN ΛCDM

A more indicative evolutionary history for these galaxies is therefore provided by the broad range of simulations tracing the growth of initial perturbations consistent with the measured anisotropies in the cosmic microwave background. This study has evolved considerably over the past decade, as each new set of observations has pushed the formation of galaxies to progressively higher redshifts. The first generation of simulations (Barkana & Loeb 2001; Miralda-Escudé 2003; Bromm & Larson 2004; Ciardi & Ferrara 2005; Glover 2005; Greif et al. 2007; Wise & Abel 2008; Salvaterra, Ferrara & Dayal 2011; Greif et al. 2012; Jaacks, Nagamine & Choi 2012) began to

★ E-mail: melia@physics.arizona.edu

Table 1. *JWST* highest-redshift galaxies and their derived properties.

Name	z^a	log(M/M$_\odot$)	SFR (M$_\odot$ yr^{-1})	Stellar age^b (Myr)	Reference
1. S5-z17 − 1	$16.66^{+1.86}_{-0.34}$	$8.8^{+0.8}_{-0.5}$	$9.7^{+30.7}_{-6.2}$	–	Harikane et al. (2023)
2. CEERS-93316	$16.4^{+0.1}_{-0.1}$	$9.0^{+0.4}_{-0.5}$	$10.0^{+10}_{-6.8}$	20^{+40}_{-10}	Donnan et al. (2023), Harikane et al. (2023), Naidu et al. (2022b)
3. S5-z12 − 1	$13.72^{+0.86}_{-1.92}$	$8.1^{+1.3}_{-0.3}$	$2.2^{+15.5}_{-1.0}$	–	Harikane et al. (2023)
4. WHL0137-5021	$12.8^{+1.1}_{-12.5}$	$8.53^{+0.18}_{-0.32}$	$5.1^{+1.9}_{-1.1}$	58^{+35}_{-35}	Bradley et al. (2022)
5. WHL0137-5124	$12.8^{+1.9}_{-12.4}$	$8.65^{+0.20}_{-0.30}$	$6.9^{+3.2}_{-1.9}$	59^{+35}_{-37}	Bradley et al. (2022)
6. GLASS-z13	12.4 ± 0.2	$9.0^{+0.3}_{-0.4}$	7^{+4}_{-3}	71^{+32}_{-33}	Castellano et al. (2022), (Harikane et al. (2023), Naidu et al. (2022a)
7. GLASS-z12 − 1	$12.22^{+0.04}_{-0.11}$	$8.6^{+0.8}_{-0.4}$	$3.0^{+11.3}_{-0.6}$	–	Castellano et al. (2022), Donnan et al. (2023), Harikane et al. (2023)
8. Maisie's Galaxy	$11.8^{+0.2}_{-0.3}$	$8.5^{+0.29}_{-0.44}$	$2.1^{+4.8}_{-2.0}$	18^{+18}_{-9}	Finkelstein et al. (2022), Harikane et al. (2023)
9. GN-z11^c	$11.09^{+0.08}_{-0.12}$	9.0 ± 0.4	24 ± 10	40^{+60}_{-34}	Oesch et al. (2016)
10. GLASS-z11	10.6 ± 0.3	9.4 ± 0.3	12^{+9}_{-4}	111^{+43}_{-54}	Castellano et al. (2022), Donnan et al. (2023), Harikane et al. (2023), Naidu et al. (2022a)
11. WHL0137-3407	$10.5^{+1.0}_{-10.5}$	$8.78^{+0.17}_{-0.33}$	$7.3^{+2.5}_{-1.2}$	70^{+50}_{-44}	Bradley et al. (2022)
12. WHL0137-5347	$10.2^{+0.9}_{-9.7}$	$9.01^{+0.21}_{-0.37}$	$14.6^{+5.8}_{-3.5}$	62^{+54}_{-43}	Bradley et al. (2022)
13. WHL0137-5330	$10.0^{+1.1}_{-7.9}$	$8.77^{+0.15}_{-0.26}$	$6.4^{+2.6}_{-1.8}$	83^{+52}_{-48}	Bradley et al. (2022)

^{a}Photometric redshift (with 2σ uncertainties) for the WHL sources calculatedusing the Calzetti et al. (2000) dust law. GLASS, CEERS, and Maisie's Galaxy redshifts (with 1σ uncertainties) were fit with the EAZY code (Brammer, van Dokkum & Coppi 2008).
^{b}Mass-weighted age of the current luminous stars, when available.
^{c}Discovered by *HST* prior to *JWST*.

elucidate how the first (Pop III) stars probably formed by redshift $z \sim 20$, nestled in the core of dark matter haloes with mass $M_{\rm halo} \sim 10^6$ M$_\odot$ (Haiman, Thoul & Loeb 1996; Tegmark et al. 1997; Abel, Bryan & Norman 2002; Bromm, Coppi & Larson 2002). This delay after the big bang resulted from the combined influence of several processes, including the initial gravitational collapse of the dark matter perturbations and the subsequent inefficient, radiative cooling of the primordial gas. The baryonic matter cooled and condensed into stars only after enough molecular hydrogen accumulated to enhance the energy loss rate (Galli & Palla 1998; Omukai & Nishi 1998). In the standard model, the Universe would have been ∼180 Myr old at redshift 20. But not all of the haloes and their baryonic content would necessarily have taken this long to condense. The more recent simulations (Haslbauer et al. 2022; Inayoshi et al. 2022; Kannan et al. 2022; Keller et al. 2023; Yajima et al. 2022; Mirocha & Furlanetto 2023; Whitler et al. 2023), in particular, show that the haloes could have been distributed across this age, some appearing perhaps as early as ∼120 Myr after the big bang (more on this below).

A typical baryonic gas cloud could subsequently have formed a protostar at the center of its halo host, eventually growing to become a > 100 M$_\odot$ main-sequence (Pop III) star (Kroupa 2002; Chabrier 2003). This is where a second major difficulty emerges, however. The ultraviolet radiation from such massive stars would have destroyed all of the H_2 in the original condensation, suggesting that most of the minihaloes likely contained – at most – only a handful of Pop III stars (Yoshida, Omukai & Hernquist 2008). Thus, many of these early structures were probably not the galaxies we see today. Nevertheless, a sufficiently broad distribution of Pop III masses could have included many below ∼ 100 M$_\odot$, whose impact on the star formation would have been less severe (Haslbauer et al. 2022; Inayoshi et al. 2022; Kannan et al. 2022; Keller et al. 2023; Yajima et al. 2022; Mirocha & Furlanetto 2023; Whitler et al. 2023).

The outpouring of radiative and mechanical energy from this first phase of stellar formation would have reheated and expelled the surrounding gas, further delaying the formation of additional stars until the plasma had time to cool again and condense to high densities. The time for this gas re-incorporation would have been another ∼100 Myr, i.e. roughly the dynamical time for a first-galaxy halo to assemble (Yoshida, Bromm & Hernquist 2004; Johnson, Greif & Bromm 2007). And now, the Universe was almost 300 Myr old.

To its credit, this scenario does provide a plausible explanation for the size of the observed galaxies. It suggests that a critical mass of > 10^8 M$_\odot$, along with an implied virial temperature >10^4 K, would have allowed atomic line emission to cool the condensing gas (Wise & Abel 2007), and recollect and mix all components of the previously shocked plasma (Greif et al. 2007). In other words, at least the mass inferred for the earliest *JWST* galaxies (Table 1) is consistent with this theoretical understanding.

But in the context of these simulations, there's no getting around the fact that the appearance of ∼ 10^9 M$_\odot$ galaxies at $z \sim 16$–17, if confirmed spectroscopically, would create a significant problem. One needs a billion new stars to have formed in only ∼70–90 Myr by the time the Universe was only $t \sim 230$ Myr old. None of the calculations to date have been able to account for the formation of galaxies at this redshift, when the expelled, hot gas had not re-cooled and re-condensed yet.

This tension between the theoretical and observational timelines has motivated the introduction of additional features and physical

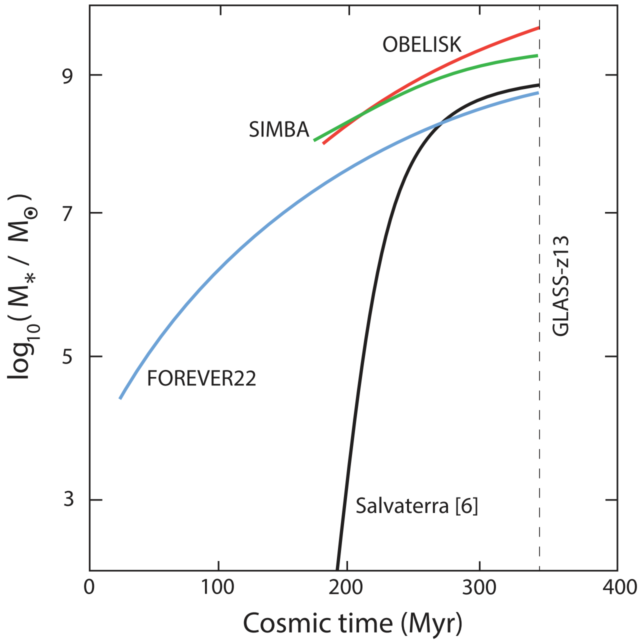

Figure 1. Comparison of galaxy growth curves with four different simulations for GLASS-z13 (line 6 in Table 1), with a final stellar mass $M_* \sim 10^9$ M$_\odot$: Salvaterra [6] corresponding to trajectory [6] in Fig. 2; FOREVER22 (Yajima et al. 2022); SIMBA (Keller et al. 2023); and OBELISK (Keller et al. 2023). The vertical dashed line indicates the age of this galaxy (∼345 Myr) in the context of *Planck*-ΛCDM.

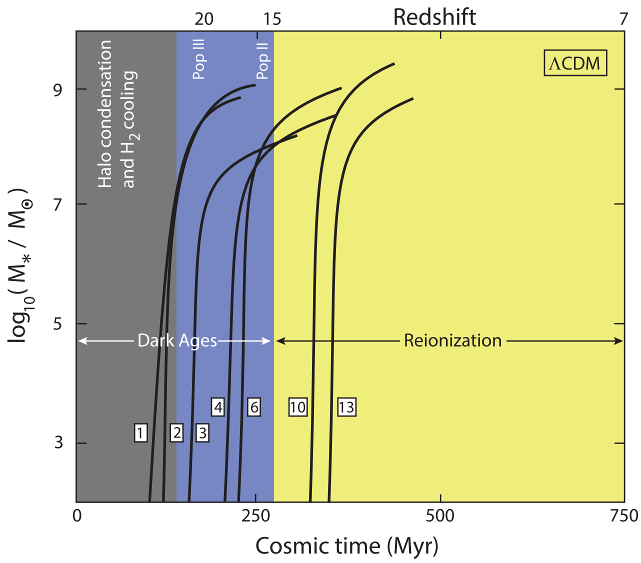

Figure 2. Growth of stellar mass in the high-z galaxy candidates discovered by *JWST* at $10 < z < 16$, as a function of cosmic time t, in ΛCDM. The principal epochs are (i) the initial halo condensation and cooling due to molecular hydrogen. This epoch typically extended over the period 0.4 Myr $\lesssim t \lesssim$ 180 Myr, but could have been as short as ∼120 Myr for some of the objects; (ii) the formation of the first Pop III stars at $t \sim$ 120–180 Myr, i.e. $z \gtrsim 20$ in this model, (iii) the transition to Pop II star formation at $t \lesssim$ 280 Myr, and the observed Epoch of Reionization (EoR) from $z \sim 15$ down to 6 (i.e. 280 Myr $< t <$ 927 Myr). These galaxy growth trajectories are primarily based on the observed SFRs and the hydrodynamical simulations in Jaacks et al. (2012), cross-checked with independent and alternative calculations in Salvaterra et al. (2011). The labels on the curves correspond to the catalogue listings in Table 1.

processes designed to mitigate the disagreement as much as possible (Haslbauer et al. 2022; Inayoshi et al. 2022; Kannan et al. 2022; Keller et al. 2023; Yajima et al. 2022; Mirocha & Furlanetto 2023; Whitler et al. 2023). For example, in their most detailed simulations to date, Yajima et al. (2022) and Keller et al. (2023) have demonstrated that the large scatter in cooling times and the presence of systems with weaker Pop III supernovae that expel far less of the condensed baryonic gas (Kitayama & Yoshida 2005; Frebel & Norris 2015) would have allowed galaxies observed by *JWST* at $z \lesssim 14$ to still have formed in the context of ΛCDM.

Kannan et al. (2022) have shown that a variable stellar initial mass function may also have produced some galaxies earlier than previously thought. A top-heavy stellar mass distribution appears to have a similar effect (Inayoshi et al. 2022), while different star formation histories could reduce the actual stellar masses of the galaxy candidates, thereby partially alleviating the tension (Haslbauer et al. 2022). Mirocha & Furlanetto (2023) suggest that at least three modifications to the *HST*-calibrated models would help lessen the tension: (i) the adoption of halo mass-independent star formation rate (SFR) efficiencies; (ii) a substantial scatter in galaxy SFRs at fixed halo masses; and (iii) the non-trivial effects of dust, both on the inferred *JWST* colours and on the produced stellar masses and ages. Finally, Whitler et al. (2023) conclude that the tension may be eased if young stellar populations formed in these early galaxies on top of older stellar populations.

Nevertheless, even with all of these modifications, the predicted galaxy masses at $z \lesssim 14$ appear to fall short of those observed by factors of a few. And they are significantly smaller than those of the galaxy candidates at $z \sim$ 16–17. Thus, if the *JWST* highest redshift sources are eventually confirmed, even the more optimistic recent simulations would be unable to explain their origin.

The four galaxy growth curves in Fig. 1 compare the time required to reach the inferred stellar mass of GLASS-z13 (the sixth entry in Table 1) by $t \sim 345$ Myr (corresponding to its redshift $z \sim 12.4$), based on four of the main simulations discussed above. For the sake of giving ΛCDM the most optimal evolutionary outcome, we shall adopt the Salvaterra et al. (2011) and Jaacks et al. (2012) frameworks which, though not as detailed and nuanced as the more recent work, predict a shorter growth time once star formation is initiated, thus making it easier to fit the observed galaxies within the ΛCDM timeline.

The various factors discussed above may now be seen more quantitatively with the simulated galaxy growth trajectories shown in Fig. 2, which also includes several critical epochs in ΛCDM. We assume that the *JWST* galaxy candidates in Table 1 followed a history of growth like those of Salvaterra et al. (2011) and Jaacks et al. (2012) at $z \sim 8$, except that their cosmic time t is suitably translated to match the redshift at which they are observed. This is justified by the fact that t is actually the proper time in the comoving frame, and the Birkhoff theorem ensures that the local growth rate was not overly affected by the cosmic expansion exterior to the bound system (Weinberg 1972; Melia 2020). In other words, once a galaxy halo becomes gravitationally bound and star formation is initiated, its evolution thereafter should be roughly translationally invariant in t.

In the Salvaterra et al. (2011) simulations, the doubling time [i.e. the inverse of the specific star formation rate (sSFR), defined as the stellar mass created per unit time per billion solar masses] and the evolutionary time at which the galaxy is observed, appears to be universally equal to ∼0.1–0.3. By comparison, the Jaacks et al. (2012) calculations show that the SFR for high-z galaxies is 'bursty,' with an average value between $z \sim 15$ and $z \sim 6$ following an exponentially increasing function with characteristic timescale $t_c \sim 70$–200 Myr, scaling with stellar mass in the range $10^6\,\mathrm{M}_\odot < M_* < 10^{10}\,\mathrm{M}_\odot$. The trajectories plotted in Fig. 2 follow this exponential growth, using the observed galaxy mass and redshift to fix the end points. Given that the sSFRs probably fluctuated during their evolution (Furtak et al. 2023; Whitler et al. 2023), we take an average of the star formation rates quoted in Table 1, i.e. $\langle \mathrm{sSFR}\rangle \sim 12.4\ \mathrm{Gyr}^{-1}$, as a fiducial value for each galaxy.

The overall impression one gets from this illustration is that the new *JWST* high-z galaxies, if confirmed, would not be consistent with the standard picture in ΛCDM. The previously growing tension developing at $z \sim 12$ has now become a more serious discordance at $z \sim 16$–17. There does not appear to be any possibility with our current physical theories of explaining how a billion-solar mass aggregate of stars could have condensed even before the primordial gas was allowed to cool and form most of the very first Pop III, and any of the Pop II, populations. In this regard, our conclusion concerning the implausibility of forming the *JWST* high-z galaxies in the context of ΛCDM is fully consistent with the findings of an alternative approach to this problem (Boylan-Kolchin 2022), based on the use of the Sheth–Tormen (Sheth & Tormen 1999) mass function to determine the abundance of massive haloes at high redshifts (Wang, Gao & Meng 2022).

3 THE TIMELINE IN $R_\mathrm{h} = ct$

But previous comparative tests between ΛCDM and a theoretically more advanced version, known as the $R_\mathrm{h} = ct$ universe (Melia & Shevchuk 2012; Melia 2020), have already hinted at the possibility that the age–redshift relation in the latter may be a better match to the Universe's evolutionary history than that in the former. For example, ΛCDM has considerable difficulty accounting for the seeding and growth of billion-solar mass black holes by redshift $z \sim 7$–8, while the timeline in $R_\mathrm{h} = ct$ matches them very well (Melia 2013, 2018c). A more complete description of this model, including its theoretical foundation and a comparison of its predictions with the data, may be seen in Melia (2018b, 2020). A review of the current problems with the standard model, pointing to a need for further development, e.g. as suggested by $R_\mathrm{h} = ct$, is provided in Melia (2022).

One of the essential features of $R_\mathrm{h} = ct$ that distinguishes it from ΛCDM is its expansion factor, $a(t) \propto t$, which results in the simple age-redshift relation $1 + z = t_0/t$ in terms of the current age, t_0 of the Universe. In this cosmology, the gravitational radius R_h is equivalent to the Hubble radius $c/H(t)$ (Melia 2018a), so $t_0 = 1/H_0$. Thus, if for simplicity we use the same Hubble constant as ΛCDM, we find that $t_0 \approx 14.5$ Gyr. The *JWST* galaxy trajectories recalculated with these relations are displayed in Fig. 3, along with the correspondingly adjusted temporal phases. The EoR redshift range $6 < z < 15$ here corresponds to 906 Myr $< t <$ 2.07 Gyr. That is, the Dark Ages ended at $t \sim 906$ Myr, providing ample time for the Universe to assemble billion-solar mass galaxies once Pop III and Pop II stars started forming in numbers. Very tellingly, all of the high-z galaxy candidates discovered so far appear towards the end of the dark ages, where one would expect them to be if they contributed – perhaps even dominated – the reionization process. In this model, one would need to find a billion-solar mass galaxy at $z \sim 50$ to run into a similar age–redshift inconsistency as that in ΛCDM.

4 CONCLUSION

The time compression problem in the standard model has been worsening for several years. Attempts at remedying the situation with the premature formation of supermassive black holes have

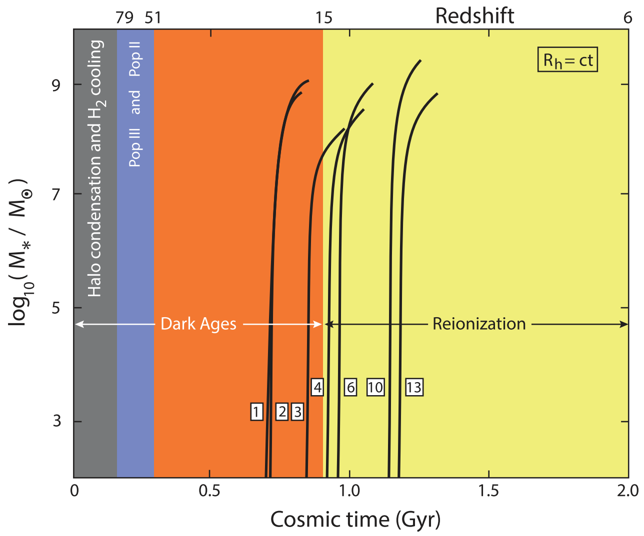

Figure 3. Same as Fig. 2, except now for the $R_\mathrm{h} = ct$ universe. The EoR here corresponds to 906 Myr $< t <$ 2.07 Gyr, and the Dark Ages extend up to ∼906 Myr. The first Pop III stars emerged at $z \gtrsim 79$ and the transition to Pop II stars occurred at $z \sim 51$. The extended period between the onset of Pop II star formation and the appearance of the first *JWST* galaxies (shown here in red) is absent in Fig. 2. In this cosmology, the *JWST* galaxy candidates are seen towards the end of the dark ages, where one would expect them to be if they were responsible for re-ionizing the intergalactic medium. Most importantly, all of these primordial galaxies would have started their growth *well after* the transition from Pop III to Pop II star formation had been completed at ∼280 Myr.

focused on two principal modifications: (i) the creation of massive (i.e. $\sim 10^5\,\mathrm{M}_\odot$) seeds; and (ii) super-Eddington accretion rates. The first of these is still speculative because it requires the collapse of an essentially zero angular momentum, optically thick, radiation-dominated plasma, which would have experienced substantial support from its internal pressure (Melia 2009); the second appears to have been ruled out by measurements suggesting that the most distant quasars are accreting at or below their Eddington rate (Willott et al. 2010; De Rosa et al. 2011; Mortlock et al. 2011).

The *JWST* discovery of high-z galaxy candidates may have worsened this timing problem considerably if their redshifts are confirmed spectroscopically, because billion-solar mass structures must have formed in only ∼70–90 Myr in some cases, and even prior to formation of the very first stars in others. The simulations completed to date in the context of ΛCDM have difficulty accounting for this outcome at $z \sim 17$, reinforcing the view that the standard model may not be able to account for the formation of structure at cosmic dawn, if the redshifts of these candidate galaxies are confirmed spectroscopically.

Instead, the timeline predicted by the $R_\mathrm{h} = ct$ cosmology would fit the birth and growth of both high-z quasars and galaxies very well, adding to the growing body of evidence supporting the introduction of the zero active mass condition from general relativity as an indispensible modification to ΛCDM.

Of course, there are still at least two ways out of this dilemma. First, the *JWST* candidate galaxies at $z \gtrsim 14$ may simply be mis-identified sources at lower redshifts. According to Furtak et al. (2023), only about half of the high-z galaxy photometric redshifts may be safely ruled out as low-z interlopers. The other half, including those of the most distant candidates, still await spectroscopic confirmation. Secondly, it is possible that we may be missing something in the basic theory, and this caveat cannot be ignored. The initial cooling of the primordial gas may have been due to something other than molecular hydrogen. An unknown process may have permitted the plasma to cool more efficiently, allowing Pop III stars to form even earlier than $t \sim 120$–180 Myr.

Certainly, the most recent simulations of Yajima et al. (2022) and Keller et al. (2023) indicate that such a process permitting the formation of Pop III stars as early as $\lesssim$100 Myr would lessen the tension with the $z \sim 16$–17 galaxies in ΛCDM. This may not completely resolve the problem, but would go a long way to mitigating the overall disagreement between the *JWST* observations and the standard model. Future simulations will probe such possibilities in even greater detail, perhaps uncovering a solution based on new physics in ΛCDM. As of today, however, the *JWST* discoveries – if confirmed – would support the timeline in $R_{\rm h} = ct$, but not in ΛCDM.

ACKNOWLEDGEMENTS

I am very grateful to the anonymous referee for a detailed and very constructive review, which has led to significant improvements in the manuscript.

DATA AVAILABILITY

No new data were generated or analysed in support of this research.

REFERENCES

Abel T., Bryan G. L., Norman M. L., 2002, Science, 295, 93
Barkana R., Loeb A., 2001, Phys. Rep., 349, 125
Behroozi P., Silk J., 2018, MNRAS, 477, 5382
Boylan-Kolchin M., 2022, preprint (arXiv:2208.01611)
Bradley L. D. et al., 2022, preprint (arXiv:2210.01777)
Brammer G. B., van Dokkum P. G., Coppi P., 2008, ApJ, 686, 1503
Bromm V., Coppi P. S., Larson R. B., 2002, ApJ, 564, 23
Bromm V., Larson R. B., 2004, ARA&A, 42, 79
Calzetti D., Armus L., Bohlin R. C., Kinney A. L., Koornneef J., Storchi-Bergmann T., 2000, ApJ, 533, 682
Castellano M. et al., 2022, ApJL, 938, L15
Chabrier G., 2003, PASP, 115, 763
Ciardi B., Ferrara A., 2005, Space Sci. Rev., 116, 625
De Rosa G., Decarli R., Walter F., Fan X., Jiang L., Kurk J., Pasquali A., Rix H. W., 2011, ApJ, 739, 56
Donnan C. T. et al., 2023, MNRAS, 518, 6011
Finkelstein S. L. et al., 2022, ApJL, 940, L55
Frebel A., Norris J. E., 2015, ARA&A, 53, 631
Furtak L. J., Shuntov M., Atek H., Zitrin A., Richard J., Lehnert M. D., Chevallard J., 2023, MNRAS, 519, 3064
Galli D., Palla F., 1998, A&A, 335, 403
Glover S., 2005, Space Sci. Rev., 117, 445
Greif T. H., Bromm V., Clark P. C., Glover S. C. O., Smith R. J., Klessen R. S., Yoshida N., Springel V., 2012, MNRAS, 424, 399
Greif T. H., Johnson J. L., Bromm V., Klessen R. S., 2007, ApJ, 670, 1
Haiman Z., Thoul A. A., Loeb A., 1996, ApJ, 464, 523
Harikane Y. et al., 2023, ApJS, 265, 5
Haslbauer M., Kroupa P., Zonoozi A. H., Haghi H., 2022, ApJ, 939, L31
Inayoshi K., Harikane Y., Inoue A. K., Li W., Ho L. C., 2022, ApJ, 938, L10
Jaacks J., Nagamine K., Choi J. H., 2012, MNRAS, 427, 403
Johnson J. L., Greif T. H., Bromm V., 2007, ApJ, 665, 85
Kannan R. et al., 2022, preprint (arXiv:2210.10066)
Keller B. W. et al., 2023, ApJL, 943, L28
Kitayama T., Yoshida N., 2005, ApJ, 630, 675
Kroupa P., 2002, Science, 295, 82
Melia F., 2009, High-Energy Astrophysics. Princeton Univ. Press, New York
Melia F., 2013, ApJ, 764, 72
Melia F., 2014, AJ, 147, 120
Melia F., 2018a, Am. J. Phys., 86, 585
Melia F., 2018b, MNRAS, 481, 4855
Melia F., 2018c, A&A, 615, A113
Melia F., 2020, The Cosmic Spacetime. Taylor and Francis, Oxford
Melia F., 2022, PASP, 134, 121001
Melia F., Shevchuk A. S. H., 2012, MNRAS, 419, 2579
Miralda-Escudé J., 2003, Science, 300, 1904
Mirocha J., Furlanetto S. R., 2023, MNRAS, 519, 843
Mortlock D. J. et al., 2011, Nature, 474, 616
Naidu R. P. et al., 2022a, ApJL, 940, L14
Naidu R. P. et al., 2022b, preprint (arXiv:2208.02794)
Oesch P. A. et al., 2016, ApJ, 819, 129
Omukai K., Nishi R., 1998, ApJ, 508, 141
Planck Collaboration VI, 2020, A&A, 641, A6
Pontoppidan K. M. et al., 2022, ApJ, 936, L14
Robertson B. E. et al., 2022, preprint (arXiv:2212.04480)
Salvaterra R., Ferrara A., Dayal P., 2011, MNRAS, 414, 847
Sheth R. K., Tormen G., 1999, MNRAS, 308, 119
Tegmark M., de Oliveira-Costa A., Devlin M. J., Netterfield C. B., Page L., Wollack E. J., 1997, ApJ, 474, L77
Treu T. et al., 2022, ApJ, 935, 110
Wang Q., Gao L., Meng C., 2022, MNRAS, 517, 6004
Weinberg S., 1972, Gravitation and Cosmology: Principles and Applications of the General Theory of Relativity. John Wiley and Sons, New York
Whitler L., Endsley R., Stark D. P., Topping M., Chen Z., Charlot S., 2023, MNRAS, 519, 157
Willott C. J. et al., 2010, AJ, 139, 906
Wise J. H., Abel T., 2007, ApJ, 665, 899
Wise J. H., Abel T., 2008, ApJ, 685, 40
Yajima H., Abe M., Fukushima H., Ono Y., Harikane Y., Ouchi M., Hashimoto T., Khochfar S., 2022, preprint (arXiv:2211.12970)
Yoshida N., Bromm V., Hernquist L., 2004, ApJ, 605, 579
Yoshida N., Omukai K., Hernquist L., 2008, Science, 321, 669